

# A COUPLED DIFFUSION-MECHANICAL LATTICE MODEL FOR THE DEGRADATION OF GRAPHITE ACTIVE PARTICLES OF LI-ION BATTERY ANODES

JORGE MARIN-MONTIN<sup>1</sup> AND FRANCISCO MONTERO-CHACÓN<sup>1</sup>

<sup>1</sup> Universidad Loyola Andalucía, Departamento de Ingeniería, Materials and Sustainability  
Avda. de las Universidades s/n, 41704 Dos Hermanas, Sevilla, Spain  
(jjmarin@uloyola.es, fpmontero@uloyola.es)

**Key words:** LIB, Active particle, graphite; porosity, Lattice model.

**Abstract.** The performance and durability of lithium-ion batteries (LIBs) are constrained by the degradation mechanisms that take place during charge and discharge cycles. Degradation of active particles (APs) of LIBs is a complex problem involving several physical phenomena (e.g., diffusion, mechanical deformation, heat transfer, to cite a few). During lithium insertion and extraction cycles, volume changes in the AP result in high mechanical stresses and, consequently, mechanical damage that promotes capacity fade.

In this work, we present a microscale 3D finite element model that takes into account the coupled effects between lithium diffusion and mechanical stress within the AP. Using the surface of an ellipsoid as the base for the geometrical construction, we are able to generate different shapes of APs, with both concave and convex surfaces. Porosity and other types of defects that may be present inside the AP are explicitly modeled, and different volume fractions, shapes, and orientations are also accounted for. In our approach, the material is discretized into a lattice of one-dimensional elements: we consider beam elements for the mechanical problem, while in the diffusive approach, the material is treated as an assembly of “nanopipes” through which the flow of Li-ions takes place. The same lattice network is used for both simulations. We follow a classical lattice model approach to characterize the fracture behavior of a single AP of a LIB anode when subjected to charge/discharge cycles. The material of the APs analyzed in this work is graphite, which presents a brittle, disordered material structure, making it suitable for lattice modeling. The mechanical problem is solved, obtaining the crack patterns associated with specific charge and discharge strategies and potential initial defects.

The simulation results correctly reproduce the experimental observations on mechanical stresses and the evolution of damage. This lattice model framework analyzing the degradation in the APs of LIBs (durability) can be used to provide more information regarding the microstructural evolution, morphological changes, and mechanical degradation in APs and identify improvement strategies.

## 1 INTRODUCTION

Nowadays, one of the greatest challenges facing the electric power industry is how to deliver the energy in a useable form, as a higher-value product, especially in the area of renewable

energy. By storing the power produced and releasing it during peak demand periods, energy storage can transform power into a high-value product. Among the different possible choices, the electrochemical batteries are the most suitable energy storage systems: portable devices able to deliver the stored chemical energy, as electrical energy, with high conversion efficiency, and without emissions [1–3]. There is a large variety of applications: from consumer applications to electric vehicles, photovoltaics or large-size auxiliary energy supply. The main challenges of battery production are insufficient battery performance, unknown future demands, and cost pressure [4,5]. Within this context, some of the most important goals arise such as the improvement of battery performance and durability, scalability, reduction of production costs, and reduction of environmental impacts of batteries [6–8].

In this work, we have focused on lithium-ion batteries (LIB), which currently have one of the highest energy densities of any rechargeable battery technology. And more specifically, in the active particles (AP) of the anode.

The lifetime of batteries is conditioned by mechanisms of chemo-mechanical degradation, such as the formation of microcracks within the AP, due to diffusion-induced stress (DIS), or the formation of the solid-electrolyte interphase (SEI) [9,10]. It is of critical importance to understand these degradation mechanisms, which constrains battery life [11,12]. Fracture due to diffusion-induced stress of the electrode active particles has been identified as one of the critical factors for the capacity fade. In recent years, attention has been paid to this degradation mechanism [10,13–15]. Microcracks are formed when the intercalation-induced stress in the active particles exceeds the fracture limit of the material. The formation of cracks and their propagation through the particle leads to an increase in the formation of SEI and a consequent decrease in available Li-ions in the loading/unloading cycles. Determining the stress level within the AP is essential to be able to estimate the evolution of mechanical degradation.

Several studies have focused on stress generation and fracture in LIBs active particles. Christensen and Newman developed pioneering work on determining the distribution of mechanical stress within carbonaceous anode material [14]. They analyzed the effect of hydrostatic stress and volume expansion during Li-ion intercalation within spherical APs. Several particle sizes, lithium insertion rates, and external pressure were considered. Zhang et al. proposed a thermal analogy model to calculate DIS in spherical and ellipsoidal shape particles [16]. Cheng and Verbrugge presented analytical solutions to evaluate the stress within a spherical AP under galvanostatic or potentiostatic conditions [17]. Barai and Mukherjee presented a lattice spring-based numerical methodology to estimate the initiation, nucleation, and propagation of microcracks within graphite active particles. Their model permits obtaining the evolution of lithium concentration and successive mechanical degradation [18].

In most of the models that study degradation in APs, simple shapes (sphere, ellipsoids, or combinations of both) are usually considered. However, real particles have a multitude of convex and concave surfaces, which generate stress concentrations during cycles, where the fracture process is most likely to begin [19]. In this work, random APs are generated, in order to capture the effect of the geometric characteristics on intercalation stresses of particles which may lead to damage.

In this study, we have focused on graphite AP of LIB anodes. Graphite has traditionally been used as active material in the anode of LIBs. And today it is still used in most commercial LIBs, despite the continuous search for alternatives that could improve energy or power density, and at the same time, capable of maintaining good stability in dis/charge cycles. Several aspects

remain to be understood regarding the de/lithiation mechanism, the reactions occurring at the electrode/electrolyte interface, and the factors limiting the rapid intercalation of lithium-ions into the graphite.

This work aims at using numerical methods to analyze the mechanical degradation within the active particles of LIBs, for different porosity types and porosity ratios, and particle shapes. A numerical framework has been developed to capture the initiation and propagation of microstructural damage and its impact on the diffusion of Li-ions within active particles. This methodology is based on the lattice model, where the continuum is replaced by a lattice of beam elements. This kind of model was introduced to model the fracture processes in brittle materials such as cement paste, mortar, concrete, and rocks [20-21].

## **2 LATTICE MODEL FRAMEWORK**

### **2.1 General formulation of the problem**

Fracture due to diffusion-induced stress of electrode active particles has been investigated through numerical means, focused on the material level, at the microscale. We have set a framework to capture the initiation and propagation of damage within AP. Initially, the distribution of Li-ion concentration inside the particle is obtained by solving the diffusion equation modeling the transport of Li-ions inside graphite, as a single-phase diffusion process. Then, mechanical stress within the particle due to the contraction/expansion caused by the de/lithiation process is calculated. As a main assumption, mechanical damage is used to explain the degradation behavior of materials due to micro-damage, and it is coupled to the diffusive damage. In this work, we are not considering associated heat transfer phenomena.

The numerical framework used in this work is the so-called lattice model, a discrete modeling technique, which presents an alternative to continuum models for fracture analysis of brittle and disordered materials. The material subject of our study is graphite of electrode active particles, which is a brittle material appropriate to be analyzed using the lattice model.

### **2.2 Spatial discretization**

In the lattice model, the domain is discretized by a network of beam elements, forming a lattice, whose nodes are placed as follows: the domain is divided into cubic cells and then, a sub-cell is defined inside each cell. A node is randomly placed in every sub-cell. The randomness of the mesh is defined by the ratio between the size of sub-cell and cell. Finally, a Delaunay tessellation of the set of nodes is performed to obtain the final lattice network.

It is important to assign the correct cross-sectional area of the lattice elements [22]. In this work, this value has been calibrated by fitting the simulation results to the analytical solution of a representative problem (i.e. expansion/contraction of a sphere subjected to external pressure).

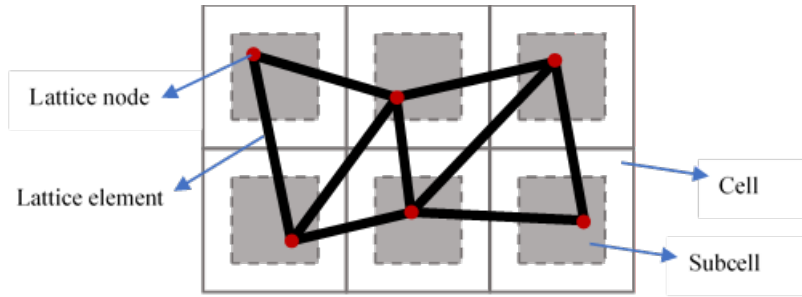


**Figure 1:** 2-D node-placement procedure and Delaunay tessellation

In the mechanical lattice approach, in order to study the mechanical degradation of the AP, Euler-Bernoulli beam elements with shear correction are used. In the diffusive lattice approach, to analyze the diffusion of lithium inside the active particle, the material is treated as an assembly of one-dimensional “nanopipes”, through which the flow takes place. The diffusion of ions takes place within the solid medium. For this reason, the same lattice mesh for both simulations is used.

### 2.3 Generation of particles

Graphite active particles have been traditionally modeled as spherical-like particles. However, it is well known that the shape of the particle influences the global behavior of the material. In this work, we analyze the effect of the shape on the fracture properties. We are considering three types of shapes, which are the most representative, depending on the natural or synthetic origin of the graphite particles: spherical and two ellipsoidal shapes, one of them with a flaky shape (Figure 2a).

There are mesopores inside the Active Particles, that change the Li-ion transport mechanism, and diffusion induced stress. Porosity and other types of defects that may be present inside the AP are explicitly modeled to understand their effect on the diffusive and mechanical degradation process. In this case, we consider three types of porosity (Figure 2b):

- 1) Concentrated porosity defect.
- 2) Scattered porosity 1: microspheres.
- 3) Scattered porosity 2: microflakes.

In all these cases, with different volume fractions of pores (0, 2.5, 5, 7.5 and 10%).

In order to generate realistic shapes of APs, we use the surface of an ellipsoid as the base for the geometrical construction, to create random graphite APs. Several random points on the surface of the ellipsoid can be chosen as the vertices of the convex polyhedron (Figure 1 (c)):

$$\begin{cases} x_i = a \sin \varphi_i \cos \theta_i \\ y_i = b \sin \varphi_i \sin \theta_i \\ z_i = c \cos \varphi_i \end{cases} \quad (1)$$

being  $a$ ,  $b$  and  $c$  are the semiaxes of the wrapping ellipsoid, with angles:

$$\begin{cases} \theta_i = \frac{2\pi}{n} + \delta \frac{2\pi}{n} (2\eta - 1) \quad \forall i = 1, \dots, n \\ \varphi_i = 2\pi\eta \quad \forall i = 1, \dots, n \end{cases} \quad (2)$$

where  $\eta$  and  $\delta$  are random numbers between 0 and 1.

We consider polyhedral of 40 vertices in our numerical simulations.

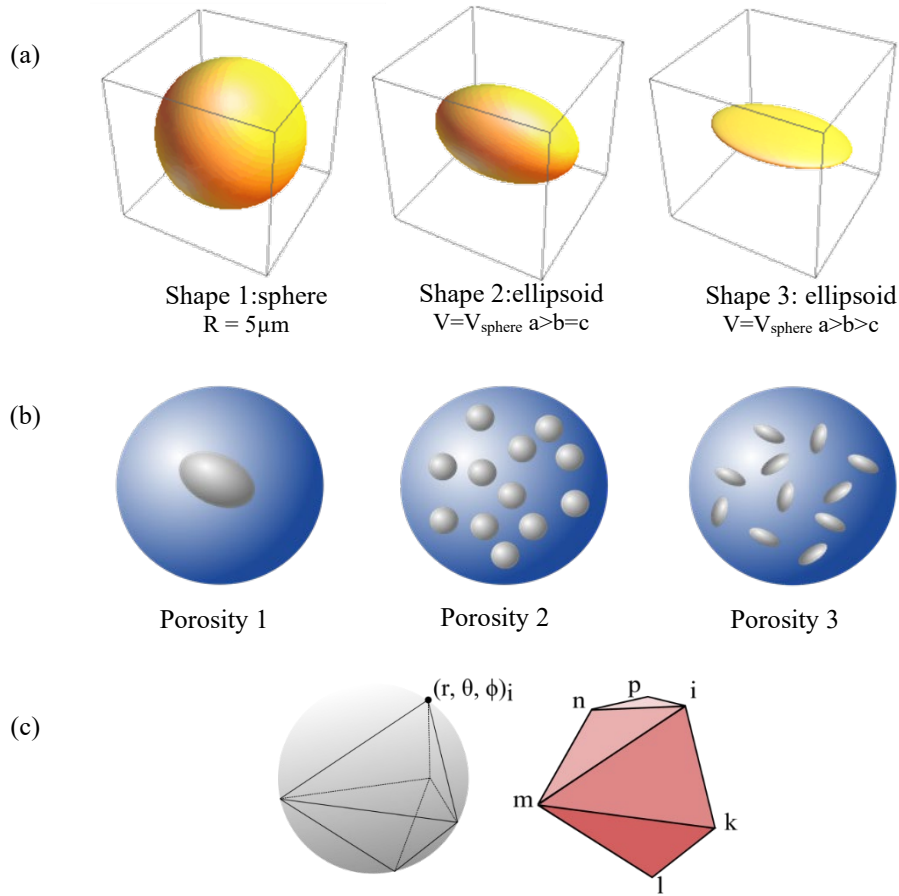


**Figure 2:** Generation of particles: (a) Shapes, (b) types of porosity analyzed, (c) convex polyhedron

## 2.4 Numerical Scheme

The numerical scheme in order to solve the coupled diffusive and mechanical problem is described in this section. For each time step: firstly, the diffusive problem is solved. Once the Li-ion concentration in the active particle has been calculated, diffusive forces applied to the lattice elements are obtained. Then, these element forces are applied to solve the mechanical problem. The damage parameter is computed, and, finally, the mechanical and diffusion matrices are updated.

### Diffusive problem

The diffusion process in the active material is described as follows [15]:

$$\frac{\partial c}{\partial t} = -\nabla \cdot \mathbf{J} \quad (3)$$

where  $c$  represents the concentration of lithium ions in the AP and  $\mathbf{J}$  is de diffusion flux. For simplification, it is assumed that there is no of stress gradients effects on the lithium ions flux. According to Fick's law, the diffusion flux is proportional to the concentration gradient:

$$\mathbf{J} = -D\nabla c \quad (4)$$

where  $D$  is the diffusion coefficient.

Combining Eqs. (3) and (4), and assuming a constant diffusion coefficient:

$$\frac{\partial c}{\partial t} = D\nabla^2 c \quad (5)$$

The initial boundary condition is:

$$c = c_0 \quad (6)$$

And, at the outer boundary, we impose the species flux:

$$\mathbf{J} = \frac{i_n}{F} \mathbf{n} \quad (7)$$

where  $i_n$  is the current density and  $F$  is Faraday's constant. The Butler-Volmer equation, establishes that the reaction current density on the electrode surfaces is a function of the exchange current density and the overpotential. In this study, we consider galvanostatic conditions instead.

### Mechanical problem

The brittle damage constitutive model is used within the lattice model framework. This model describes degradation of a material due to micro-cracking with the aid of a single scalar damage parameter  $d_m$ , growing from zero (undamaged state) to one (completely damaged state).

The stress-strain relationship is represented by the Eq. (8):

$$\boldsymbol{\sigma} = (1 - d_m)\mathbf{D}_0^{el} : \boldsymbol{\varepsilon}^{el} \quad (8)$$

$$\boldsymbol{\varepsilon}^{el} = \boldsymbol{\varepsilon} - \boldsymbol{\varepsilon}^d \quad (9)$$

$$\boldsymbol{\varepsilon}^d = \tilde{c}\Omega\mathbf{I} \quad (10)$$

where  $\mathbf{D}_0^{el}$  is the stiffness tensor,  $\tilde{c} = c - c_0$  is the change in the Li-ion concentration from the initial value (stress-free status), and  $\Omega$  is the partial molar volume of the active material.

Failure criterion requires the comparative stress in the lattice beam element is smaller than its strength. The lattice beam element stress (note it is a scalar) is computed by Eq. (11) from internal forces applying beam theory. If it is greater than the maximum allowable tensile stress, the mechanical damage  $d_m$  is set to 1.

$$\sigma_{eq-Lattice\ beam} = \alpha_N \frac{F}{A} + \alpha_M \frac{(|M_i|, |M_j|)_{max}}{W} \quad (11)$$

where, for each lattice beam element,  $F$  is the axial force in the lattice beam element,  $A$  is the cross-sectional area of the element,  $M_i$ , and  $M_j$  are the bending moments,  $W$  is the cross-sectional modulus for bending resistance, and  $\alpha_N$  and  $\alpha_M$  are the normal force and the bending influence factor in the fracture criterion. Typical values are  $\alpha_N=1$  and  $\alpha_M=0$ .

To describe the evolution of the diffusive damage parameter, a power law could be assumed, as well as other types of laws that are adjusted according to experimental results.

Stiffness matrix updates following Eqs (12).

$$\mathbf{K}_m = (1 - d_m)\mathbf{K}_{m,0} \quad (12)$$

where  $\mathbf{K}_{m,0}$  is the undamaged stiffness matrix.

### 3 RESULTS

Different particle shapes (shape 1: sphere,  $R=5\ \mu\text{m}$ ; shape 2: ellipsoid, semi-axes:  $a>b=c$ ,  $V_{\text{ellipsoid}}=V_{\text{sphere}}$ ; shape 3: ellipsoid, semi-axes:  $a>b>c$ ,  $V_{\text{ellipsoid}}=V_{\text{sphere}}$ ), different porosity types (one concentrated defect; scattered porosity 1: *microspheres*; scattered porosity 2: *microflakes*), and porosity ratios (0, 2.5, 5, 7.5 and 10%) were analyzed to study their effects on the fracture behavior of the active particle. The material properties of graphite used in the simulations are listed in Table 1. For simplification,  $E$ ,  $\nu$ ,  $D$  of graphite is assumed to remain constant.

**Table 1:** Material properties of graphite anode active particle

Property	Unit	$\text{Li}_x\text{C}_6$	Reference
Young's module ( $E$ )	GPa	15	[23]
Poisson's ratio ( $\nu$ )		0.3	[23]
Diffusion coefficient ( $D$ )	$\text{m}^2\cdot\text{s}^{-1}$	$7.08 \times 10^{-15}$	[23]
Partial molar volume ( $\Omega$ )	$\text{m}^3\cdot\text{mol}^{-1}$	$3.60 \times 10^{-6}$	[23]
Maximum Li-ion concentration ( $c_{\text{max}}$ )	$\text{mol}\cdot\text{m}^{-3}$	$2.29 \times 10^4$	[23]
Maximum allowable tensile stress (MPa)	MPa	87.5	[24]

#### 3.1 Diffusive Problem

Figure 3 shows the results of lithium-ion concentration during lithiation, at different time steps. In this first simulation, no mechanical damage is considered. The particle is spherical, with no porosity. It can be seen that the surface of the particle exhibits the higher lithium-ion concentration, whereas the inner area exhibited lower concentration. The concentration profile evolves as the simulation progresses smoothing the concentration gradient within the particle.

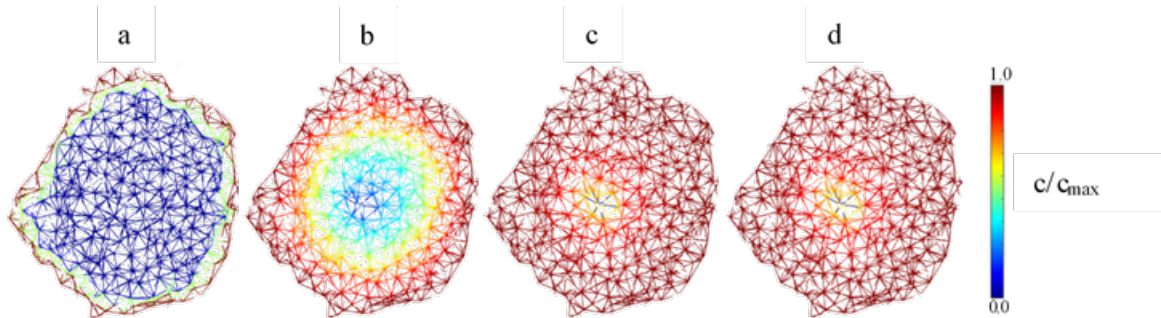


**Figure 3:** Concentration of Li-ion within a particle (Spherical shape, no porosity) at different time steps. Cross-section shown. Time step: (a) 1, (b) 100, (c) 100, (d) 1000 s.

Applying these concentration results, the diffusion-induced stress due to Li insertion (during charge) is computed at different time steps. The outer region of the active particle expands as Li-ions are inserted, producing a strain difference between the outer and the inner regions of the particle. As result, the stress (normal stress in the lattice element) during the lithiation is tensile at the center of the particle, but compressive at the surface, due to the expansion during lithium insertion. Maximum tensile stress value at the center of the particle increases over time

(Fig. 4a).

In the opposite way, diffusion-induced stress due to Li extraction (during discharge) is computed at different time steps. In the opposite way to the previous case, during the delithiation, the stress is compressive at the center of the particle, but tensile at the surface. The maximum value of stress is located at the center of the particle (Fig. 4b).

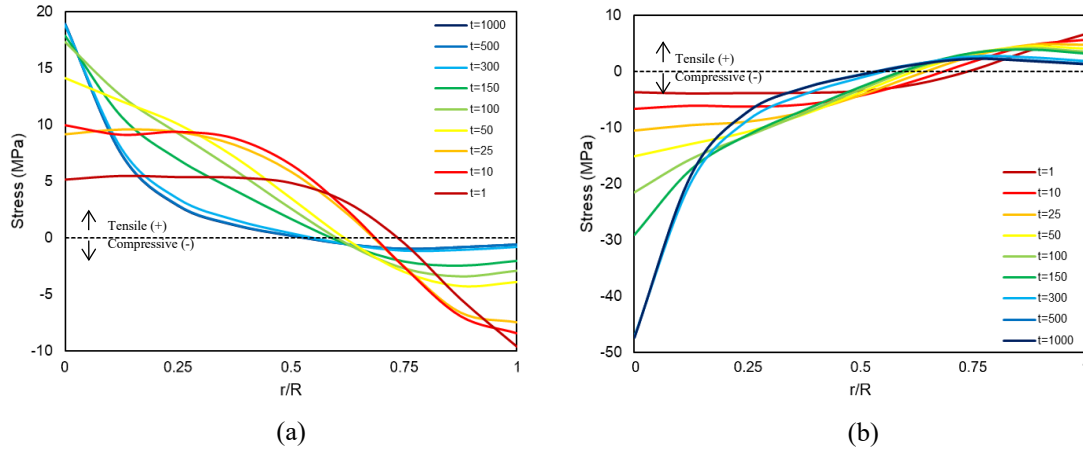


**Figure 4:** Stress profile during (a) lithiation and (b) delithiation at different time steps

### 3.2 Coupled Mechanical-Diffusive Problem

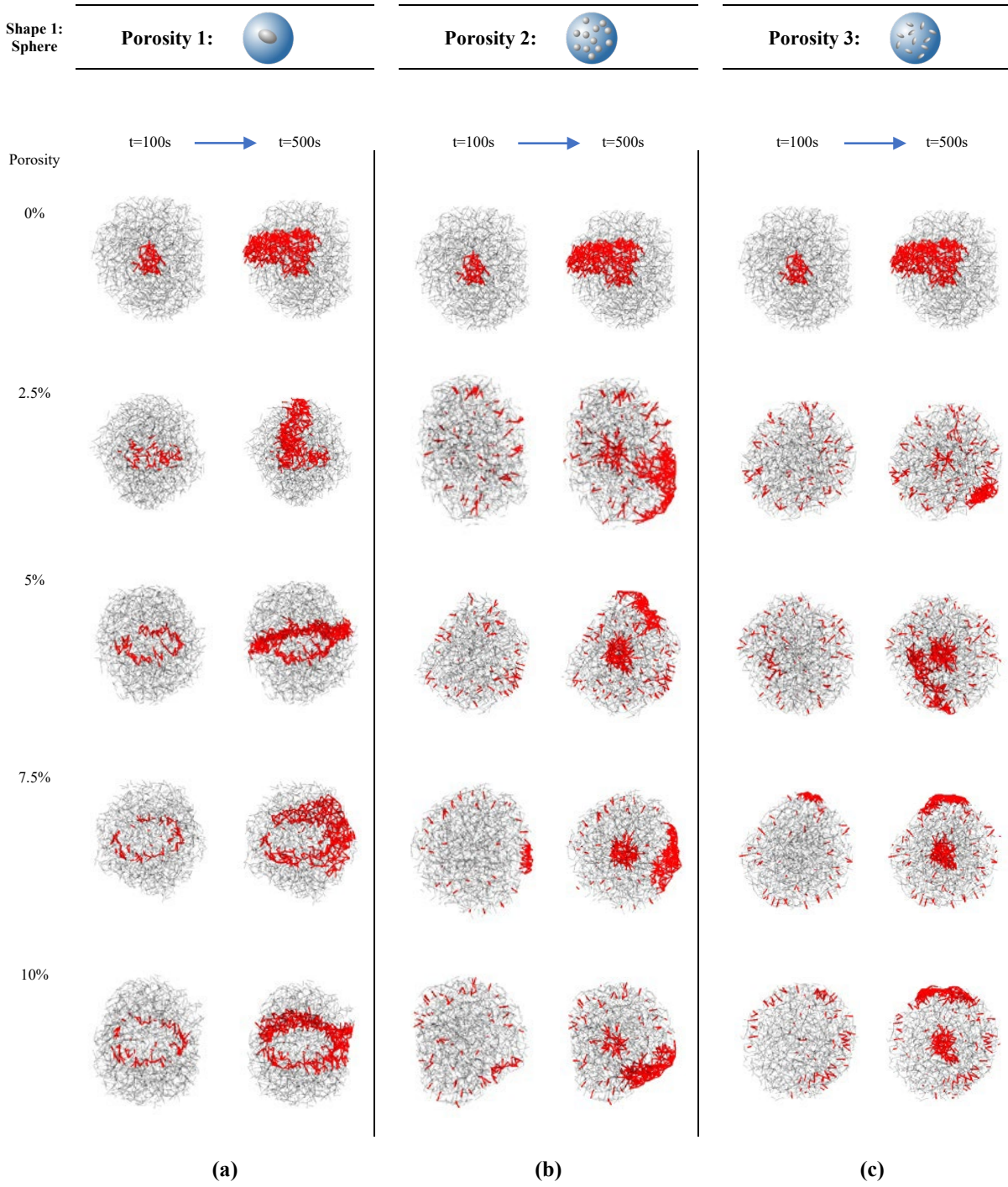
Diffusion-induced stress may cause damage within the particle if the stress surpasses the fracture limit of the material. The results shown in this section try to give a qualitative idea of the evolution of mechanical damage in an active particle, due to DIS. Also, we show the influence of the shape of the particle and the type of porosity in the different patterns cracking.

Figure 5 shows the mechanical damage propagation inside the active particle, due to diffusion-induced stress in the coupled mechanical-diffusive problem, during lithiation.

Figure 5a shows the results for the spherical shape, and porosity type 1, for different porosity values and at two different time steps. Red solid lines represent damaged elements within the lattice mesh. The results show that first, a few microcracks are initiated around the center part of the particle, and then the microcracks spread further towards the outer surface. The most likely point of fracture during Li insertion is at the center of the particle because crack initiation is more likely due to tension.

Figures 5b and 5c show the same results for the case of porosity type 2 and 3, respectively. Comparisons can be made to learn the influences of the porosity type on the simulated problem. Some differences exist at the beginning of the lithiation when the damage is distributed much more dispersed throughout the particle. The results are in agreement with the experimental results, although we cannot ignore the effect of the mechanical boundary conditions inside the particle.





**Figure 5:** Mechanical damage during lithiation at different time steps, spherical shape, porosity:0-10%. Porosity type: (a) one concentrated defect; (b) scattered porosity 1: *microspheres*; (c) scattered porosity 2: *microflakes*

Figure 6 shows the mechanical damage distribution in case of ellipsoidal shape and flake

shape. Porosity types are compared at the same time steps. It can be seen that the microcracks are more localized in spherical shape than in the ellipsoidal one. Less localized microcracks patterns are observed in shape 3.

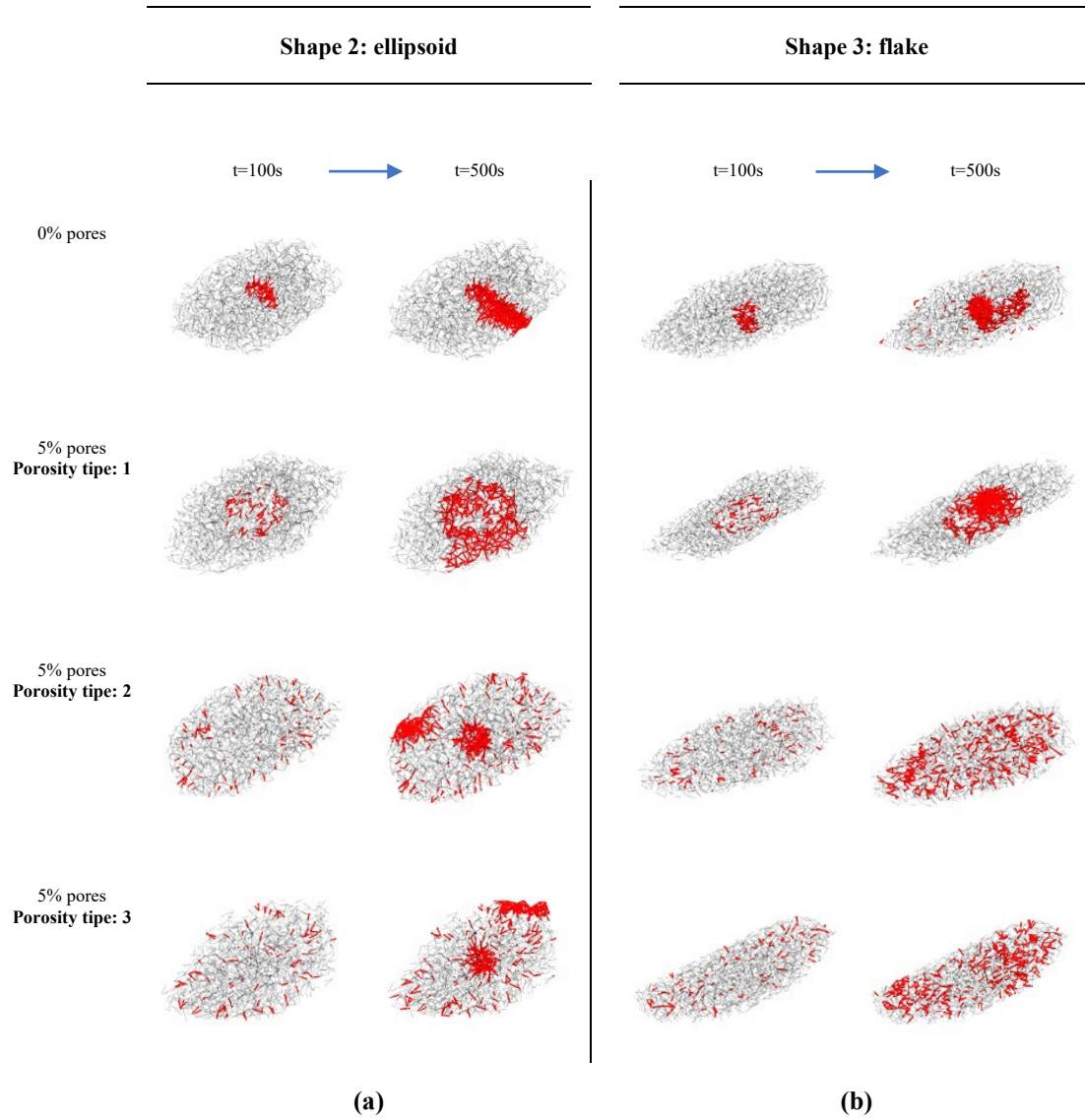


**Figure 6:** Mechanical damage during lithiation at different time steps. (a) Shape 2: ellipsoid. (b) Shape 3; flake. Porosity = 0 and 5%.

#### 4 CONCLUSIONS

In this work we have presented a novel approach to the characterization of active particles performance in Li-ion battery anodes. In our approach, we are able to generate 3D virtual

microstructures that not only take into account different geometrical aspects of the particles (e.g., shape, convexity), but also allows the inclusion of inter- and intragranular defects. These microstructures are then subject to diffusion and mechanical analyses to understand better the role of imperfections in the degradations of this type of particles.

For the simulation of the physical phenomena (ion diffusion and deformation), we have used a 3D lattice model, consisting of 1D elements that represent the internal microstructure of the material. In the diffusion problems, these elements are equivalent to “nanopipes” through which Li ions transport through the material, while in the case of the mechanical problems, are beams that represent the mechanical interaction between different points in the material. This approach also allows for the simulation of crack initiation and propagation. In this sense, the mechanical damage variable is used to explain the degradation behavior of graphite due to micro-damage, and it is coupled to the diffusive damage.

The results obtained with our model are in accordance with the literature, especially in the mechanical stress distribution and evolution of damage.

Future works include coupling this material-level simulation to the characterize their behavior in components (i.e., electrodes) through a multiscale.

## ACKNOWLEDGMENTS

This work was partially funded by the Consejería de Economía, Conocimiento, Empresas y Universidad (Junta de Andalucía), under the project grant PY18-RE-0023, “Multiscale, multiphysics simulation platform for virtual design of batteries: The VirtualBats Project”.

## REFERENCES

- [1] B. Dunn, H. Kamath, and J.-M. Tarascon, “Electrical Energy Storage for the Grid: A Battery of Choices System power ratings, module size.” *Science* 334(2011) 928-935.
- [2] B. Scrosati and J. Garche, “Lithium batteries: Status, prospects and future,” *J. Power Sources*, vol. 195, no. 9. pp. 2419–2430, May 01, 2010, doi: 10.1016/j.jpowsour.2009.11.048.
- [3] S. Chu and A. Majumdar, “Opportunities and challenges for a sustainable energy future,” *Nature*, vol. 488, no. 7411. pp. 294–303, Aug. 16, 2012, doi: 10.1038/nature11475.
- [4] T. Tsujikawa, K. Yabuta, M. Arakawa, and K. Hayashi, “Safety of large-capacity lithium-ion battery and evaluation of battery system for telecommunications,” *Journal of Power Sources*, vol. 244, pp. 11–16, 2013, doi: 10.1016/j.jpowsour.2013.01.155.
- [5] B. Nykvist and M. Nilsson, “Rapidly falling costs of battery packs for electric vehicles,” *Nature Climate Change*, vol. 5, no. 4, pp. 329–332, Mar. 2015, doi: 10.1038/nclimate2564.
- [6] M. Marinaro *et al.*, “Bringing forward the development of battery cells for automotive applications: Perspective of R&D activities in China, Japan, the EU and the USA,” *Journal of Power Sources*, vol. 459, May 2020, doi: 10.1016/j.jpowsour.2020.228073.
- [7] R. Wagner, N. Preschitschek, S. Passerini, J. Leker, and M. Winter, “Current research trends and prospects among the various materials and designs used in lithium-based batteries,” *J. Applied Electrochemistry*, vol. 43, 5, pp. 481–496, May 01, 2013.
- [8] S.-I. Tobishima, K. Takei, Y. Sakurai, and J.-I. Yamaki, “Lithium ion cell safety,” *J. Power Sources* 90, 188–195 (2000)

- [9] P. Arorat, R. E. White, and M. Doyle, “Capacity Fade Mechanisms and Side Reactions in Lithium-Ion Batteries.” *Journal of the Electrochemical Society*, 145(10) 3647-3667, 1998.
- [10] R. Deshpande, Y.-T. Cheng, M. W. Verbrugge, and A. Timmons, “Diffusion Induced Stresses and Strain Energy in a Phase-Transforming Spherical Electrode Particle,” *Journal of The Electrochemical Society*, vol. 158, no. 6, p. A718, 2011, doi: 10.1149/1.3565183.
- [11] J. W. Fergus, “Recent developments in cathode materials for lithium ion batteries,” *Journal of Power Sources*, vol. 195, no. 4, pp. 939–954, Feb. 15, 2010, doi: 10.1016/j.jpowsour.2009.08.089.
- [12] J.-M. Tarascon and M. Armand, “Issues and challenges facing rechargeable lithium batteries,” 2001. *Nature* 414, 359–367 (2001).
- [13] Y.-T. Cheng and M. W. Verbrugge, “Diffusion-Induced Stress, Interfacial Charge Transfer, and Criteria for Avoiding Crack Initiation of Electrode Particles,” *Journal of The Electrochemical Society*, vol. 157, no. 4, p. A508, 2010, doi: 10.1149/1.3298892.
- [14] J. Christensen and J. Newman, “Stress generation and fracture in lithium insertion materials,” *Journal of Solid State Electrochemistry*, vol. 10, no. 5, pp. 293–319, May 2006, doi: 10.1007/s10008-006-0095-1.
- [15] R. Grantab and V. B. Shenoy, “Pressure-Gradient Dependent Diffusion and Crack Propagation in Lithiated Silicon Nanowires,” *Journal of The Electrochemical Society*, vol. 159, no. 5, pp. A584–A591, 2012, doi: 10.1149/2.072205jes.
- [16] X. Zhang, W. Shyy, and A. Marie Sastry, “Numerical Simulation of Intercalation-Induced Stress in Li-Ion Battery Electrode Particles,” *Journal of The Electrochemical Society*, vol. 154, no. 10, p. A910, 2007, doi: 10.1149/1.2759840.
- [17] Y. T. Cheng and M. W. Verbrugge, “The influence of surface mechanics on diffusion induced stresses within spherical nanoparticles,” *Journal of Applied Physics*, vol. 104, no. 8, 2008, doi: 10.1063/1.3000442.
- [18] P. Barai and P. P. Mukherjee, “Stochastic Analysis of Diffusion Induced Damage in Lithium-Ion Battery Electrodes,” *Journal of The Electrochemical Society*, vol. 160, no. 6, pp. A955–A967, 2013, doi: 10.1149/2.132306jes.
- [19] C. Lim, B. Yan, L. Yin, and L. Zhu, “Simulation of diffusion-induced stress using reconstructed electrodes particle structures generated by micro/nano-CT,” *Electrochimica Acta*, vol. 75, pp. 279–287, Jul. 2012, doi: 10.1016/j.electacta.2012.04.120.
- [20] E. Schlangen and J. G. M. van Mier, “Simple lattice model for numerical simulation of fracture of concrete materials and structures,” *Materials and Structures* 25, 534–542 (1992). <https://doi.org/10.1007/BF02472449>.
- [21] E. Schlangen and E. J. Garboczi, “Fracture simulations of concrete using lattice models: Computational aspects,” *Engineering Fracture Mechanics*, vol. 57, no. 2–3, pp. 319–332, 1997, doi: 10.1016/s0013-7944(97)00010-6.
- [22] J. E. Bolander and N. Sukumar, “Irregular lattice model for quasistatic crack propagation,” *Physical Review B - Condensed Matter and Materials Physics*, vol. 71, no. 9, Mar. 2005.
- [23] Y. Zhang and Z. Guo, “Numerical computation of central crack growth in an active particle of electrodes influenced by multiple factors,” *Acta Mechanica Sinica/Lixue Xuebao*, vol. 34, no. 4, pp. 706–715, Aug. 2018, doi: 10.1007/s10409-018-0764-1.
- [24] K. Takahashi, K. Higa, S. Mair, M. Chintapalli, N. Balsara, and V. Srinivasan, “Mechanical Degradation of Graphite/PVDF Composite Electrodes: A Model-Experimental Study,” *Journal of The Electrochemical Society*, vol. 163, no. 3, pp. A385–A395, 2016, doi: 10.1149/2.0271603jes.